Supporting Information: Topological insulators vs. topological Dirac semimetals in honeycomb compounds

Xiuwen Zhang[*,†,‡], Qihang Liu[§,‡], Qiunan Xu[♮], Xi Dai[♯], and Alex Zunger[*,‡]

[†]Shenzhen Key Laboratory of Flexible Memory Materials and Devices, College of Electronic Science and Technology, Shenzhen University, Guangdong 518060, China
[‡]Renewable and Sustainable Energy Institute, University of Colorado, Boulder, Colorado 80309, USA
[§]Department of Physics and Shenzhen Institute for Quantum Science and Technology, Southern University of Science and Technology, Shenzhen 518055, China
[♮]Beijing National Laboratory for Condensed Matter Physics, and Institute of Physics, Chinese Academy of Sciences, Beijing 100190, China
[♯]Department of Physics, The Hong Kong University of Science and Technology, Hong Kong
Keywords: density functional theory, topological insulators, topological Dirac semimetals

I. List of studied honeycomb ABX compounds

A. Classification of the ABX honeycombs according to electronic structures

Figure S1 gives the full list of studied honeycomb ABX compounds that are classified into four categories, i.e. topological insulator (TI), topological Dirac semimetal (TDSM), normal insulator, and metal, according to DFT+SOC calculated band structures and topological invariants. We considered eight ABX groups: I-II-V, I-XII-V, XI-II-V, XI-XII-V, I-I-VI, I-XI-VI, XI-I-VI, and XI-XI-VI, where I = (Li, Na, K, Rb, Cs), II = (Mg, Ca, Sr, Ba), XI = (Cu, Ag, Au), XII = (Zn, Cd, Hg), V = (N, P, As, Sb, Bi), and VI = (O, S, Se, Te). Among the 816 calculated ABX honeycombs, we find 160 TI's, 96 TDSM's, 282 normal insulators (or semiconductors) and 278 metals.

Topological Insulators (160):

AgBaAs, AgBaBi, AgBaP, AgBaSb, AgCaAs, AgCaBi, AgCaN, AgCaP, AgCaSb, AgCsS, AgCsSe, AgCsTe, AgKO, AgKS, AgKSe, AgKTe, AgLiTe, AgNaS, AgNaSe, AgNaTe, AgRbO, AgRbS, AgRbSe, AgRbTe, AgSrAs, AgSrBi, AgSrN, AgSrP, AgSrSb, AuBaAs, AuBaP, AuCaAs, AuCaBi, AuCaP, AuCaSb, AuKSe, AuKTe, AuNaTe, AuRbSe, AuRbTe, AuSrAs, AuSrBi, AuSrP, AuSrSb, BaCsAs, BaCsBi, BaCsSb, BaKBi, BaNaBi, BaRbBi, BaRbN, BaRbSb, CaCsAs, CaCsBi, CaCsP, CaCsSb, CaKAs, CaKBi, CaKSb, CaNaBi, CaRbAs, CaRbBi, CaRbN, CaRbP, CaRbSb, CdCsAs, CdCsP, CdKN, CdNaN, CdNaP, CdRbN, CsCaBi, CsCaN, CsSrBi, CuBaAs, CuBaBi, CuBaP, CuBaSb, CuCaAs, CuCaBi, CuCaN, CuCaP, CuCaSb, CuCsS, CuCsSe, CuCsTe, CuKS, CuKSe, CuKTe, CuLiTe, CuNaSe, CuNaTe, CuRbS, CuRbSe, CuRbTe, CuSrAs, CuSrBi, CuSrN, CuSrP, CuSrSb, HgCsBi, HgRbBi, KBaBi, KCaBi, KSrBi, LiBaAs, LiBaBi, LiBaSb, LiCaBi, LiSrAs, LiSrBi, LiSrSb, MgCsAs, MgCsBi, MgCsP, MgCsSb, MgKAs, MgKBi, MgKN, MgKP, MgKSb, MgNaAs,MgNaBi, MgNaN, MgNaP, MgNaSb, MgRbAs, MgRbN, MgRbP, MgRbSb, NaBaAs, NaBaBi, NaBaN, NaBaP, NaBaSb, NaCaBi, NaSrAs, NaSrBi, NaSrSb, RbBaBi, RbCaBi, RbSrBi, SrCsAs, SrCsBi, SrCsP, SrCsSb, SrKAs, SrKBi, SrKSb, SrNaBi, SrRbAs, SrRbBi, SrRbSb, ZnCsAs, ZnCsBi, ZnCsSb, ZnKN, ZnLiN, ZnNaN, ZnRbBi

Topological Dirac Semimetals (96):

AgHgP, AuAuS, AuCdN, AuHgN, AuHgP, BaAgAs, BaAgBi, BaAgN, BaAuAs, BaAuBi, BaAuN, BaAuP, BaAuSb, BaCuBi, BaCuN, BaCuSb, CaAgAs, CaAgBi, CaAgN, CaAuAs, CaAuBi, CaAuN, CaAuP, CaAuSb, CaCuBi, CaCuN, CsAgO, CsCdAs, CsCdN, CsCdSb, CsCuO, CsHgP, CsMgBi, KAuTe, KCdAs, KCdN, KCdSb, KCuO, KHgP, KMgBi, KMgN, KZnN, LiAgO, LiAgSe, LiAuSe, LiAuTe, LiCdAs, LiCdN, LiCuO, LiHgAs, LiHgN, LiHgP, MgAgAs, MgAgBi, MgAgN, MgAgSb, MgAuAs, MgAuN, MgAuP, MgCuAs, MgCuN, NaAgO, NaAgS, NaAgSe, NaAuSe, NaAuTe, NaCdAs, NaCdN, NaCdSb, NaCuO, NaCuSe, NaHgAs, NaHgP, NaMgN, NaZnN, RbAgO, RbAuTe, RbCdAs, RbCdN, RbCuO, RbHgP, RbMgBi, RbMgN, RbZnN, SrAgAs, SrAgBi, SrAgN, SrAuAs, SrAuBi, SrAuN, SrAuP, SrAuSb, SrCuBi, SrCuN, ZnAgN, ZnCuN

Normal Insulators (282):

AgAuS, AgAuSe, AgAuTe, AgHgN, AgLiS, AgZnP, BaAgP, BaKAs, BaKP, BaKSb, BaLiAs, BaLiBi, BaLiN, BaLiP, BaLiSb, BaNaAs, BaNaN, BaNaP, BaNaSb, BaRbAs, BaRbP, CaAgP, CaCuAs, CaKN, CaKP, CaLiAs, CaLiN, CaLiP, CaLiSb, CaNaAs, CaNaN, CaNaP, CsAgS, CsAgSe, CsAgTe, CsAuO, CsAuS, CsAuSe, CsBaAs, CsBaBi, CsBaP, CsBaSb, CsCaAs, CsCaP, CsCaSb, CsCdBi, CsCdP, CsCsO, CsCsS, CsCsSe, CsCsTe, CsCuS, CsCuSe, CsCuTe, CsHgAs, CsHgBi, CsHgN, CsHgSb, CsKO, CsKS, CsKSe, CsKTe, CsLiO, CsLiS, CsLiSe, CsLiTe, CsMgAs, CsMgN, CsMgP, CsMgSb, CsNaO, CsNaS, CsNaSe, CsNaTe, CsRbO, CsRbS, CsRbSe, CsRbTe, CsSrAs, CsSrP, CsSrSb, CsZnAs, CsZnBi, CsZnP, CsZnSb, CuLiS, CuNaO, KAgS, KAgSe, KAgTe, KAuO, KAuS, KAuSe, KBaAs, KBaP, KBaSb, KCaAs, KCaP, KCaSb, KCdBi, KCdP, KCsO, KCsS, KCsSe, KCsTe, KCuS, KCuSe, KCuTe, KHgAs, KHgBi, KHgN, KHgSb, KKO, KKS, KKSe, KKTe, KLiO, KLiS, KLiSe, KLiTe, KMgAs, KMgP, KMgSb, KNaO, KNaS, KNaSe, KNaTe, KRbO, KRbS, KRbSe, KRbTe, KSrAs, KSrP, KSrSb, KZnAs, KZnBi, KZnP, KZnSb, LiAgS, LiAgTe, LiAuO, LiAuS, LiBaN, LiBaP, LiCaAs, LiCaN, LiCaP, LiCsO, LiCsS, LiCsSe, LiCsTe, LiCuS, LiCuSe, LiCuTe, LiKO, LiKS, LiKSe, LiKTe, LiLiO, LiLiS, LiLiSe, LiLiTe, LiMgN, LiNaO, LiNaS, LiNaSe, LiNaTe, LiRbO, LiRbS, LiRbSe, LiRbTe, LiSrN, LiSrP, LiZnAs, LiZnN, LiZnP, LiZnSb, MgLiN, MgLiP, NaAgTe, NaAuO, NaAuS, NaCaN, NaCaP, NaCdP, NaCsO, NaCsS, NaCsSe, NaCsTe, NaCuS, NaCuTe, NaHgN, NaHgSb, NaKO, NaKS, NaKSe, NaKTe, NaLiO, NaLiS, NaLiSe, NaLiTe, NaMgAs, NaMgP, NaNaO, NaNaS, NaNaSe, NaNaTe, NaRbO, NaRbS, NaRbSe, NaRbTe, NaSrN, NaSrP, NaZnAs, NaZnBi, NaZnP, NaZnSb, RbAgS, RbAgSe, RbAgTe, RbAuO, RbAuS, RbAuSe, RbBaAs, RbBaP, RbBaSb, RbCaAs, RbCaP, RbCaSb, RbCdBi, RbCdP, RbCdSb, RbCsO, RbCsS, RbCsSe, RbCsTe, RbCuS, RbCuSe, RbCuTe, RbHgAs, RbHgBi, RbHgN, RbHgSb, RbKO, RbKS, RbKSe, RbKTe, RbLiO, RbLiS, RbLiSe, RbLiTe, RbMgAs, RbMgP, RbMgSb, RbNaO, RbNaS, RbNaSe, RbNaTe, RbRbO, RbRbS, RbRbSe, RbRbTe, RbSrAs, RbSrP, RbSrSb, RbZnAs, RbZnBi, RbZnP, RbZnSb, SrAgP, SrKN, SrKP, SrLiAs, SrLiBi, SrLiN, SrLiP, SrLiSb, SrNaAs, SrNaN, SrNaP, SrNaSb, SrRbP

Metals (278):

AgAgO, AgAgS, AgAgSe, AgAgTe, AgAuO, AgCdAs, AgCdBi, AgCdN, AgCdP, AgCdSb, AgCsO, AgCuO, AgCuS, AgCuSe, AgCuTe, AgLiO, AgLiSe, AgMgAs, AgMgBi, AgMgN, AgMgP, AgMgSb, AgNaO, AgHgAs, AgHgBi, AgHgSb, AgBaN, AgZnAs, AgZnBi, AgZnN, AgZnSb, AuAgO, AuAgS, AuAgSe, AuAgTe, AuAuO, AuAuSe, AuAuTe, AuBaBi, AuBaN, AuBaSb, AuCaN, AuCdAs, AuCdBi, AuCdP, AuCdSb, AuCsO, AuCsS, AuCsSe, AuCsTe, AuCuO, AuCuS, AuCuSe, AuCuTe, AuHgAs, AuHgBi, AuHgSb, AuKO, AuKS, AuLiO, AuLiS, AuLiSe, AuLiTe, AuMgAs, AuMgBi, AuMgN, AuMgP, AuMgSb, AuNaO, AuNaS, AuNaSe, AuRbO, AuRbS, AuSrN, AuZnAs, AuZnBi, AuZnN, AuZnP, AuZnSb, BaAgSb, BaCsN, BaCsP, BaCuAs, BaCuP, BaKN, CaAgSb, CaCsN, CaCuP, CaCuSb, CaLiBi, CaNaSb, CdAgAs, CdAgBi, CdAgN, CdAgP, CdAgSb, CdAuAs, CdAuBi, CdAuN, CdAuP, CdAuSb, CdCsBi, CdCsN, CdCsSb, CdCuAs, CdCuBi, CdCuN, CdCuP, CdCuSb, CdKAs, CdKBi, CdKP, CdKSb, CdLiAs, CdLiBi, CdLiN, CdLiP, CdLiSb, CdNaAs, CdNaBi, CdNaSb, CdRbAs, CdRbBi, CdRbP, CdRbSb, CsAuTe, CsBaN, CsSrN, CsZnN, CuAgO, CuAgS, CuAgSe, CuAgTe, CuAuO, CuAuS, CuAuSe, CuAuTe, CuBaN, CuCdAs, CuCdBi, CuCdN, CuCdP, CuCdSb, CuCsO, CuCuO, CuCuS, CuCuSe, CuCuTe, CuHgAs, CuHgBi, CuHgN, CuHgP, CuHgSb, CuKO, CuLiO, CuLiSe, CuMgAs, CuMgBi, CuMgN, CuMgP, CuMgSb, CuNaS, CuRbO, CuZnAs, CuZnBi, CuZnN, CuZnP, CuZnSb, HgAgAs, HgAgBi, HgAgN, HgAgP, HgAgSb, HgAuAs, HgAuBi, HgAuN, HgAuP, HgAuSb, HgCsAs, HgCsN, HgCsP, HgCsSb, HgCuAs, HgCuBi, HgCuN, HgCuP, HgCuSb, HgKAs, HgKBi, HgKN, HgKP, HgKSb, HgLiAs, HgLiBi, HgLiN, HgLiP, HgLiSb, HgNaP, HgNaAs, HgNaBi, HgNaN, HgNaSb, HgRbAs, HgRbN, HgRbP, HgRbSb, KAgO, KBaN, KCaN, KSrN, LiCaSb, LiCdBi, LiCdP, LiCdSb, LiHgBi, LiHgSb, LiMgAs, LiMgBi, LiMgP, LiMgSb, LiZnBi, MgAgP, MgAuBi, MgAuSb, MgCsN, MgCuBi, MgCuP, MgCuSb, MgLiAs, MgLiBi, MgLiSb, MgRbBi, NaCaAs, NaCdBi, NaCaSb, NaHgBi, NaMgBi, NaMgSb, RbBaN, RbCaN, RbSrN, SrAgSb, SrCsN, SrCuAs, SrCuP, SrCuSb, SrRbN, ZnAgAs, ZnAgBi, ZnAgP, ZnAgSb, ZnAuAs, ZnAuBi, ZnAuN, ZnAuP, ZnAuSb, ZnCsN, ZnCsP, ZnCuAs, ZnCuBi, ZnCuP, ZnCuSb, ZnKAs, ZnKBi, ZnKP, ZnKSb, ZnLiAs, ZnLiBi, ZnLiP, ZnLiSb, ZnNaAs, ZnNaBi, ZnNaP, ZnNaSb, ZnRbAs, ZnRbN, ZnRbP, ZnRbSb

Figure S1. ABX honeycombs in the four categories (topological insulator, topological Dirac semimetal, normal insulator, and metal) based on DFT+SOC band structure and topological invariant calculations. Whereas most of the listed ABX compounds do not adopt the honeycomb structure (compounds indicated in red color are stable in the honeycomb structure,[9,10] others have different structures), we have considered firstly all compounds in the honeycomb structure so as to distill chemical regularities, followed by establishing for a subset of compounds that are the most interesting, the lowest energy structure.

B. List of topological insulators with non-zero band gaps

There are 52 TIs with non-zero fundamental band gaps according to DFT+SOC, which are listed as follows with their band gaps given in parentheses (in eV):

AgCaAs(0.02), AgCaP(0.02), AgCsS(0.002), AgCsSe(0.01), AgCsTe(0.04), AgKS(0.01), AgKSe(0.05), AgKTe(0.13), AgRbS(0.01), AgRbSe(0.06), AgRbTe(0.12), CaKAs(0.05), CaKBi(0.04), CaKSb(0.01), CaRbAs(0.01), CaRbBi(0.01), CdNaN(0.01), CsCaBi(0.09), CsSrBi(0.15), CuKTe(0.10), CuRbTe(0.07), KBaBi(0.22), KCaBi(0.23), KSrBi(0.26), LiBaAs(0.05), LiBaBi(0.13), LiBaSb(0.03), LiCaBi(0.19), LiSrAs(0.03), LiSrBi(0.29), LiSrSb(0.07), MgKN(0.01), MgNaN(0.01), MgNaP(0.03), NaBaAs(0.05), NaBaBi(0.15), NaBaP(0.01), NaBaSb(0.08), NaCaBi(0.34), NaSrAs(0.05), NaSrBi(0.32), NaSrSb(0.10), RbBaBi(0.19), RbCaBi(0.23), RbSrBi(0.24), SrKAs(0.04), SrKBi(0.07), SrKSb(0.07), SrRbAs(0.06), SrRbBi(0.04), SrRbSb(0.04), ZnNaN(0.01).

C. List of topological insulators with zero band gap but non-zero direct energy gaps

There are 108 TIs with zero fundamental band gap but non-zero energy gaps between N_{th} and N_{th}+1 bands at each *k*-point (i.e. direct energy gaps) according to DFT+SOC, which are listed as follows with their direct energy gaps given in parentheses (in eV):

AgBaAs(0.15), AgBaBi(0.54), AgBaP(0.09), AgBaSb(0.27), AgCaBi(0.51), AgCaN(0.03), AgCaSb(0.23), AgKO(0.04), AgLiTe(0.17), AgNaS(0.03), AgNaSe(0.14), AgNaTe(0.27), AgRbO(0.04), AgSrAs(0.13), AgSrBi(0.53), AgSrN(0.04), AgSrP(0.04), AgSrSb(0.26), AuBaAs(0.17), AuBaP(0.09), AuCaAs(0.13), AuCaBi(0.42), AuCaP(0.06), AuCaSb(0.24), AuKSe(0.07), AuKTe(0.25), AuNaTe(0.17), AuRbSe(0.12), AuRbTe(0.17), AuSrAs(0.16), AuSrBi(0.47), AuSrP(0.06), AuSrSb(0.27), BaCsAs(0.02), BaCsBi(0.22), BaCsSb(0.03), BaKBi(0.19), BaNaBi(0.17), BaRbBi(0.20), BaRbN(0.02), BaRbSb(0.03), CaCsAs(0.10), CaCsBi(0.38), CaCsP(0.04), CaCsSb(0.18), CaNaBi(0.31), CaRbN(0.03), CaRbP(0.02), CaRbSb(0.17), CdCsAs(0.17), CdCsP(0.07), CdKN(0.05), CdNaP(0.05), CdRbN(0.03), CsCaN(0.06), CuBaAs(0.16), CuBaBi(0.54), CuBaP(0.06), CuBaSb(0.26), CuCaAs(0.12), CuCaBi(0.51), CuCaN(0.04), CuCaP(0.06),

CuCaSb(0.23), CuCsS(0.03), CuCsSe(0.13), CuCsTe(0.19), CuKS(0.02), CuKSe(0.15), CuLiTe(0.21), CuNaSe(0.09), CuNaTe(0.28), CuRbS(0.05), CuRbSe(0.15), CuSrAs(0.14), CuSrBi(0.53), CuSrN(0.05), CuSrP(0.07), CuSrSb(0.24), HgCsBi(0.15), HgRbBi(0.27), MgCsAs(0.15), MgCsBi(0.50), MgCsP(0.06), MgCsSb(0.27), MgKAs(0.14), MgKBi(0.44), MgKP(0.03), MgKSb(0.25), MgNaAs(0.12), MgNaBi(0.31), MgNaSb(0.24), MgRbAs(0.13), MgRbN(0.03), MgRbP(0.06), MgRbSb(0.26), NaBaN(0.02), SrCsAs(0.09), SrCsBi(0.34), SrCsP(0.03), SrCsSb(0.17), SrNaBi(0.29), ZnCsAs(0.17), ZnCsBi(0.43), ZnCsSb(0.28), ZnKN(0.04), ZnLiN(0.04), ZnRbBi(0.39).

D. Band gaps of the honeycomb normal insulators

The fundamental band gaps from DFT+SOC of the 282 honeycomb normal insulators listed in Fig. S1 are given below in parentheses (in eV):

AgAuS(0.14), AgAuSe(0.05), AgAuTe(0.02), AgHgN(0.001), AgLiS(0.12), AgZnP(0.001), BaAgP(0.11), BaKAs(0.22), BaKP(0.35), BaKSb(0.001), BaLiAs(0.77), BaLiBi(0.001), BaLiN(0.50), BaLiP(0.93), BaLiSb(0.50), BaNaAs(0.51), BaNaN(0.34), BaNaP(0.66), BaNaSb(0.15), BaRbAs(0.002), BaRbP(0.16), CaAgP(0.13), CaCuAs(0.002), CaKN(0.33), CaKP(0.03), CaLiAs(0.89), CaLiN(1.73), CaLiP(1.15), CaLiSb(0.18), CaNaAs(0.36), CaNaN(0.94), CaNaP(0.59), CsAgS(0.45), CsAgSe(0.24), CsAgTe(0.36), CsAuO(0.14), CsAuS(0.16), CsAuSe(0.05), CsBaAs(0.71), CsBaBi(0.03), CsBaP(0.85), CsBaSb(0.46), CsCaAs(0.33), CsCaP(0.43), CsCaSb(0.45), CsCdBi(0.39), CsCdP(0.22), CsCsO(0.72), CsCsS(2.06), CsCsSe(1.79), CsCsTe(1.52), CsCuS(0.45), CsCuSe(0.23), CsCuTe(0.42), CsHgAs(0.10), CsHgBi(0.64), CsHgN(0.08), CsHgSb(0.28), CsKO(1.17), CsKS(2.17), CsKSe(1.83), CsKTe(1.63), CsLiO(1.93), CsLiS(2.24), CsLiSe(1.91), CsLiTe(1.72), CsMgAs(0.53), CsMgN(0.38), CsMgP(0.83), CsMgSb(0.61), CsNaO(1.58), CsNaS(2.08), CsNaSe(1.75), CsNaTe(1.64), CsRbO(0.97), CsRbS(2.16), CsRbSe(1.79), CsRbTe(1.54), CsSrAs(0.10), CsSrP(0.20), CsSrSb(0.43), CsZnAs(0.15), CsZnBi(0.44), CsZnP(0.56), CsZnSb(0.13), CuLiS(0.04), CuNaO(0.01), KAgS(0.28), KAgSe(0.08), KAgTe(0.29), KAuO(0.29), KAuS(0.17), KAuSe(0.02), KBaAs(0.45), KBaP(0.64), KBaSb(0.29), KCaAs(0.72), KCaP(1.03), KCaSb(0.40), KCdBi(0.28), KCdP(0.25),

KCsO(1.29), KCsS(1.65), KCsSe(1.33), KCsTe(1.11), KCuS(0.37), KCuSe(0.15), KCuTe(0.45), KHgAs(0.06), KHgBi(0.56), KHgN(0.09), KHgSb(0.23), KKO(1.87), KKS(2.05), KKSe(1.58), KKTe(1.34), KLiO(2.53), KLiS(2.69), KLiSe(2.22), KLiTe(2.04), KMgAs(0.63), KMgP(1.03), KMgSb(0.77), KNaO(1.83), KNaS(2.22), KNaSe(1.71), KNaTe(1.49), KRbO(1.52), KRbS(1.80), KRbSe(1.40), KRbTe(1.18), KSrAs(0.46), KSrP(0.95), KSrSb(0.43), KZnAs(0.21), KZnBi(0.43), KZnP(0.84), KZnSb(0.28), LiAgS(0.07), LiAgTe(0.05), LiAuO(0.19), LiAuS(0.03), LiBaN(0.04), LiBaP(0.07), LiCaAs(0.21), LiCaN(1.17), LiCaP(0.47), LiCsO(0.36), LiCsS(0.76), LiCsSe(0.50), LiCsTe(0.36), LiCuS(0.75), LiCuSe(0.31), LiCuTe(0.45), LiKO(1.44), LiKS(1.29), LiKSe(0.85), LiKTe(0.65), LiLiO(5.08), LiLiS(3.52), LiLiSe(2.41), LiLiTe(1.78), LiMgN(1.70), LiNaO(2.28), LiNaS(1.96), LiNaSe(1.25), LiNaTe(0.99), LiRbO(0.97), LiRbS(0.95), LiRbSe(0.62), LiRbTe(0.47), LiSrN(0.33), LiSrP(0.31), LiZnAs(0.53), LiZnN(0.39), LiZnP(1.36), LiZnSb(0.12), MgLiN(2.02), MgLiP(0.47), NaAgTe(0.05), NaAuO(0.21), NaAuS(0.16), NaCaN(0.65), NaCaP(0.54), NaCdP(0.23), NaCsO(0.33), NaCsS(0.76), NaCsSe(0.49), NaCsTe(0.36), NaCuS(0.22), NaCuTe(0.38), NaHgN(0.09), NaHgSb(0.08), NaKO(1.17), NaKS(1.21), NaKSe(0.78), NaKTe(0.60), NaLiO(2.84), NaLiS(3.04), NaLiSe(2.24), NaLiTe(1.88), NaMgAs(0.44), NaMgP(1.18), NaNaO(1.53), NaNaS(1.68), NaNaSe(1.06), NaNaTe(0.85), NaRbO(0.75), NaRbS(0.92), NaRbSe(0.58), NaRbTe(0.44), NaSrN(0.03), NaSrP(0.14), NaZnAs(0.26), NaZnBi(0.06), NaZnP(1.00), NaZnSb(0.38), RbAgS(0.28), RbAgSe(0.10), RbAgTe(0.28), RbAuO(0.27), RbAuS(0.17), RbAuSe(0.04), RbBaAs(0.57), RbBaP(0.70), RbBaSb(0.35), RbCaAs(0.30), RbCaP(0.46), RbCaSb(0.35), RbCdBi(0.38), RbCdP(0.17), RbCdSb(0.002), RbCsO(1.07), RbCsS(1.76), RbCsSe(1.47), RbCsTe(1.24), RbCuS(0.28), RbCuSe(0.10), RbCuTe(0.37), RbHgAs(0.09), RbHgBi(0.64), RbHgN(0.09), RbHgSb(0.27), RbKO(1.45), RbKS(2.07), RbKSe(1.64), RbKTe(1.41), RbLiO(2.20), RbLiS(2.36), RbLiSe(1.96), RbLiTe(1.81), RbMgAs(0.49), RbMgP(0.82), RbMgSb(0.62), RbNaO(1.53), RbNaS(2.12), RbNaSe(1.70), RbNaTe(1.55), RbRbO(1.23), RbRbS(1.89), RbRbSe(1.50), RbRbTe(1.28), RbSrAs(0.54), RbSrP(1.02), RbSrSb(0.49), RbZnAs(0.10), RbZnBi(0.47), RbZnP(0.66), RbZnSb(0.17), SrAgP(0.11), SrKN(0.47), SrKP(0.31), SrLiAs(1.13), SrLiBi(0.05),

SrLiN(1.11), SrLiP(1.32), SrLiSb(0.61), SrNaAs(0.55), SrNaN(0.53), SrNaP(0.85), SrNaSb(0.13), SrRbP(0.003).

II. Theoretical methodology

A. Comparison of electronic structures from DFT and HSE

We are aware of the DFT errors on underestimating the band gaps of insulators and semiconductors. Figure S2 compares the band structures of NaCaBi, KBaBi, CaAuP, and BaAuP in the honeycomb (S1) structure from DFT and HSE [1,2] methods without considering the spin-orbit coupling (SOC) effect. NaCaBi and KBaBi are the only two stable honeycomb TI's predicted from DFT (see Fig. S1), while CaAuP and BaAuP (with the lightest anion P^{3-} among the predicted stable topological materials) are the only two stable phosphide honeycomb TDSM's predicted in this study (see Fig. S1). For NaCaBi, the HSE band structure shows analogous band inversion patterns as DFT but smaller band inversion energy due to the DFT errors. The band inversion energy (0.80 eV) from DFT (see Fig. S2a) is very close to that (0.89 eV) from DFT+SOC (see Fig. 4a). It is reasonable to expect that including SOC in HSE calculation will not increase the band inversion energy too much as well. The parity analysis of both DFT and HSE electronic structures of NaCaBi gives $Z_2 = 1$. For KBaBi, DFT electronic structure shows a band inversion with calculated $Z_2 = 1$ whereas the HSE electronic structure gives $Z_2 = 0$ with a trivial band gap. For CaAuP and BaAuP, both DFT and HSE electronic structures give $Z_2 = 1$ with the band inversion energy from HSE much smaller than that from DFT (see Fig. S2e-h). Therefore, the prediction of band inversions in the ABX materials are to-some-extent limited by the accuracy of DFT method. However, the separation between the TI and TDSM materials (the main purpose of this study) that is related to the mechanism of band-crossing/band-anti-crossing of a band-inverted compound, is not affected by the DFT errors on band gaps.

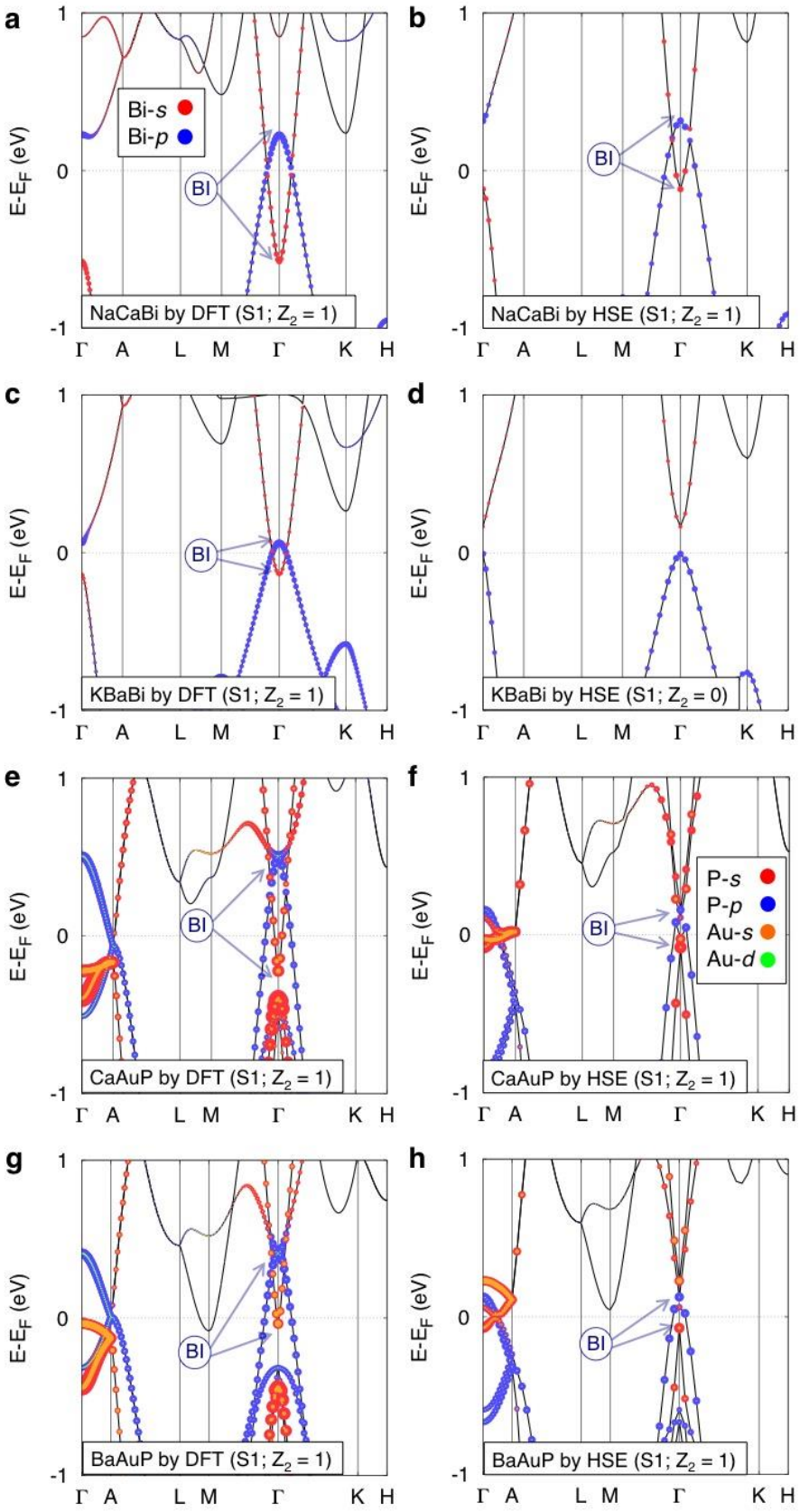

Figure S2. Electronic structures of NaCaBi (a, b), KBaBi (c, d), CaAuP (e, f) and BaAuP (g, h) in the honeycomb structure from DFT (a, c, e, g) and HSE (b, d, f, h) without SOC. The dotted lines with different colors denote the band projection onto different atomic orbitals. The band inversion is denoted by BI with arrows pointing to the inverted states.

B. Testing the effect of SOC on structural relaxation and band inversion

Table S1 compares the lattice constants of honeycomb structures relaxed from DFT (second column) and those from DFT+SOC (third column) for NaCaBi, KBaBi, CaAuP, and BaAuP, showing rather small differences between them. Figure S3 shows the band structures of the above four compounds in the honeycomb (S1) structure from DFT+SOC with crystal structures relaxed in DFT+SOC, as well as the band structure of CaAuP and BaAuP from DFT+SOC with structures relaxed in DFT for comparison. By comparing Fig. S3a *vs.* Fig. 4a, Fig. S3b *vs.* Fig. 4b, Fig. S3c *vs.* Fig. S3d, and Fig. S3e *vs.* Fig. S3f, we see that including SOC effect in structure relaxation has negligible effect on the calculated band edge states of the ABX compounds.

Table S1. Lattice constants of NaCaBi, KBaBi, CaAuP and BaAuP in the honeycomb structures relaxed using DFT+SOC or DFT.

Compound name	Lattice constants (a, c) from DFT (in nm)	Lattice constants (a, c) from DFT+SOC (in nm)
NaCaBi	(0.557, 0.678)	(0.557, 0.678)
KBaBi	(0.617, 0.757)	(0.609, 0.739)
CaAuP	(0.430, 0.795)	(0.429, 0.797)
BaAuP	(0.447, 0.918)	(0.446, 0.920)

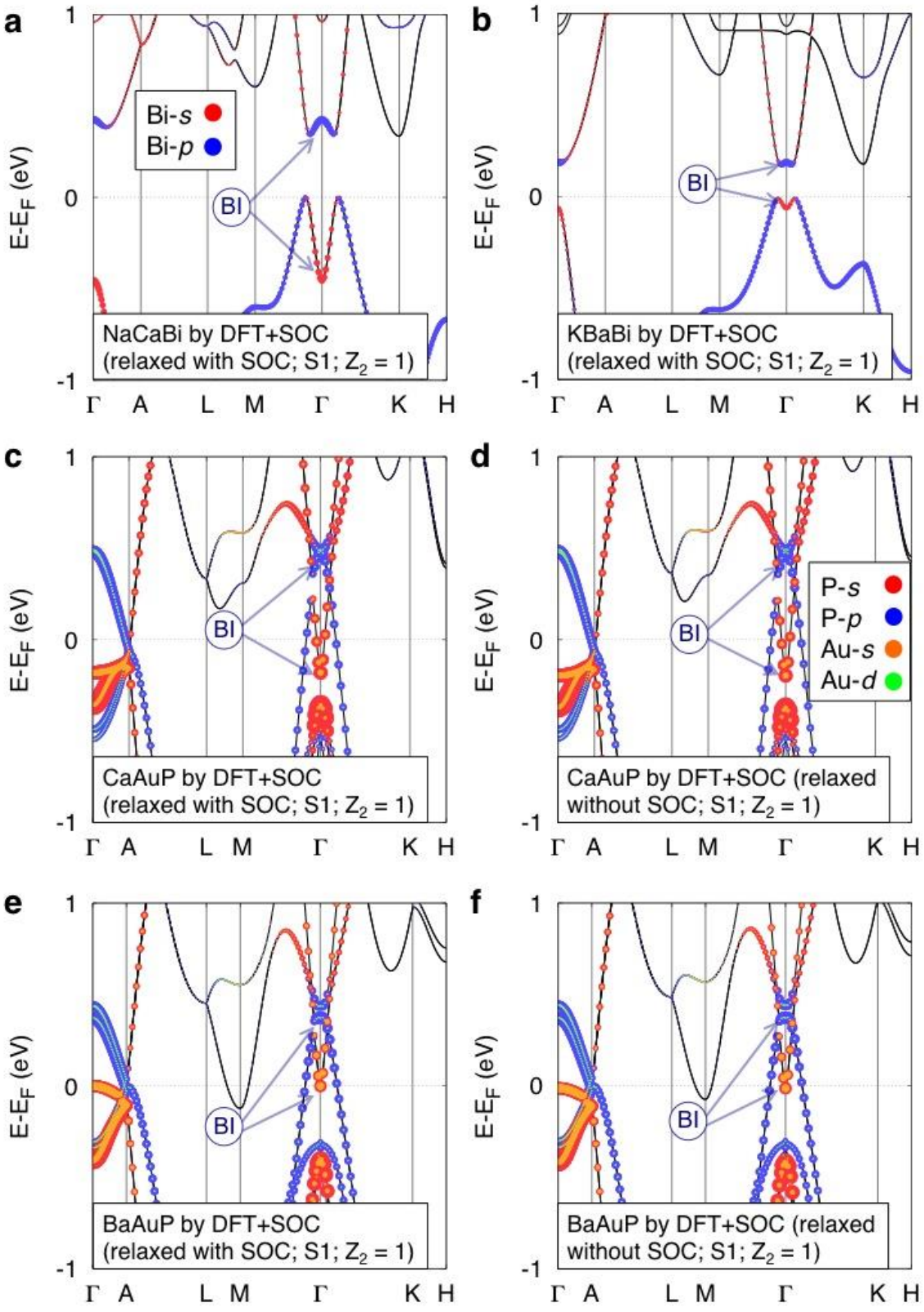

Figure S3. Electronic structures of NaCaBi (a), KBaBi (b), CaAuP (c, d) and BaAuP (e, f) in the honeycomb structure from DFT+SOC with crystal structures relaxed using DFT+SOC (a, b, c, e) or DFT (d, f). The dotted lines with different colors denote the band projection onto different atomic orbitals. The band inversion is denoted by BI with arrows pointing to the inverted states.

D. Thermodynamic stability determination

To determine the thermodynamic stability of a target ABX compound, we consider all of its possible disproportionation channels to the competing phases (elemental phases, binaries and ternaries) with neighboring compositions.[3] This is done by solving a set of inequalities in a three-dimensional space of chemical potentials $\Delta\mu_A$, $\Delta\mu_B$ and $\Delta\mu_X$. For all competing elemental phases, we used inequalities of the form $\Delta\mu_I$ (I = A, B, X) < 0. For all competing binary phases A_pB_q we used inequalities of the form $p\Delta\mu_A + q\Delta\mu_B < \Delta H_f (A_pB_q)$. For all competing ternary phases $A_pB_qX_r$ we used inequalities of the form $p\Delta\mu_A + q\Delta\mu_B + r\Delta\mu_X < \Delta H_f (A_pB_qX_r)$. This 3-dimensitonal space of chemical potentials was reduced to 2 dimensions by the $\Delta\mu_A + \Delta\mu_B + \Delta\mu_X = \Delta H_f$ (ABX) equation. The values of $\Delta\mu_A$ and $\Delta\mu_B$ where all inequalities are satisfied define the stability area of the ABX compound.[4]

E. Topological invariants characterization

For the honeycomb ($P6_3/mmc$) structure and other centrosymmetric structures considered in this study, because of the simultaneous presence of time-reversal symmetry and inversion symmetry, we use the parities of the occupied bands at TRIM point to evaluate the topological invariants.[5] For each centrosymmetric structure, we calculate the TI topological invariant Z_2 from the parity products of the occupied bands at all TRIM points. For the honeycomb ($P6_3/mmc$) structures, analogous to the case of Na_3Bi in the same space group $P6_3/mmc$,[6] we calculate the TDSM topological invariant ν_{2D} from the parity products of the occupied bands at the TRIM points in the $k_z = 0$ plane. The evaluated Z_2 and ν_{2D} values plus the band structures can be used to identify the TI and TDSM phases among the calculated compounds. In our calculations, the TDSM's ($\nu_{2D} = 1$) also have $Z_2 = 1$. For non-centrosymmetric structures, we use the method from Refs. [7,8] to calculate the topological invariant Z_2, which is based on the evolution of Wannier function centers, which is also applicable to centrosymmetric structures. We tested the above two methods on a few honeycomb ($P6_3/mmc$) structures and found that they produce the same Z_2 values.

III. Electronic structures and thermodynamic stability of representative honeycomb ABX compounds

A. Band structures of special ABX TDSM's

Figure S4 shows the electronic structures of KMgBi, RbMgBi, CsMgBi, NaMgN, KMgN, and RbMgN that are the topological materials ($Z_2 = 1$) with B = Mg, indicating that ABX honeycomb structures with B = Mg are TDSM's if band-inverted.

Figure S5 gives the band structures of CsCaN and CsCaBi that are honeycomb TI's with long *c* lattice constant as shown in Figure 1d. CsCaN and CsCaBi have very large A atom (Cs) with large polarizability that could to-some-extent maintain the strong coupling between B-X layers.

Figure S6 shows the band structure and wave function squares of band edge states of LiAuTe that was predicted to be a honeycomb TI in Ref. [9]. According to Figure S6 and our topological invariant calculations, we found that LiAuTe is a honeycomb TDSM.

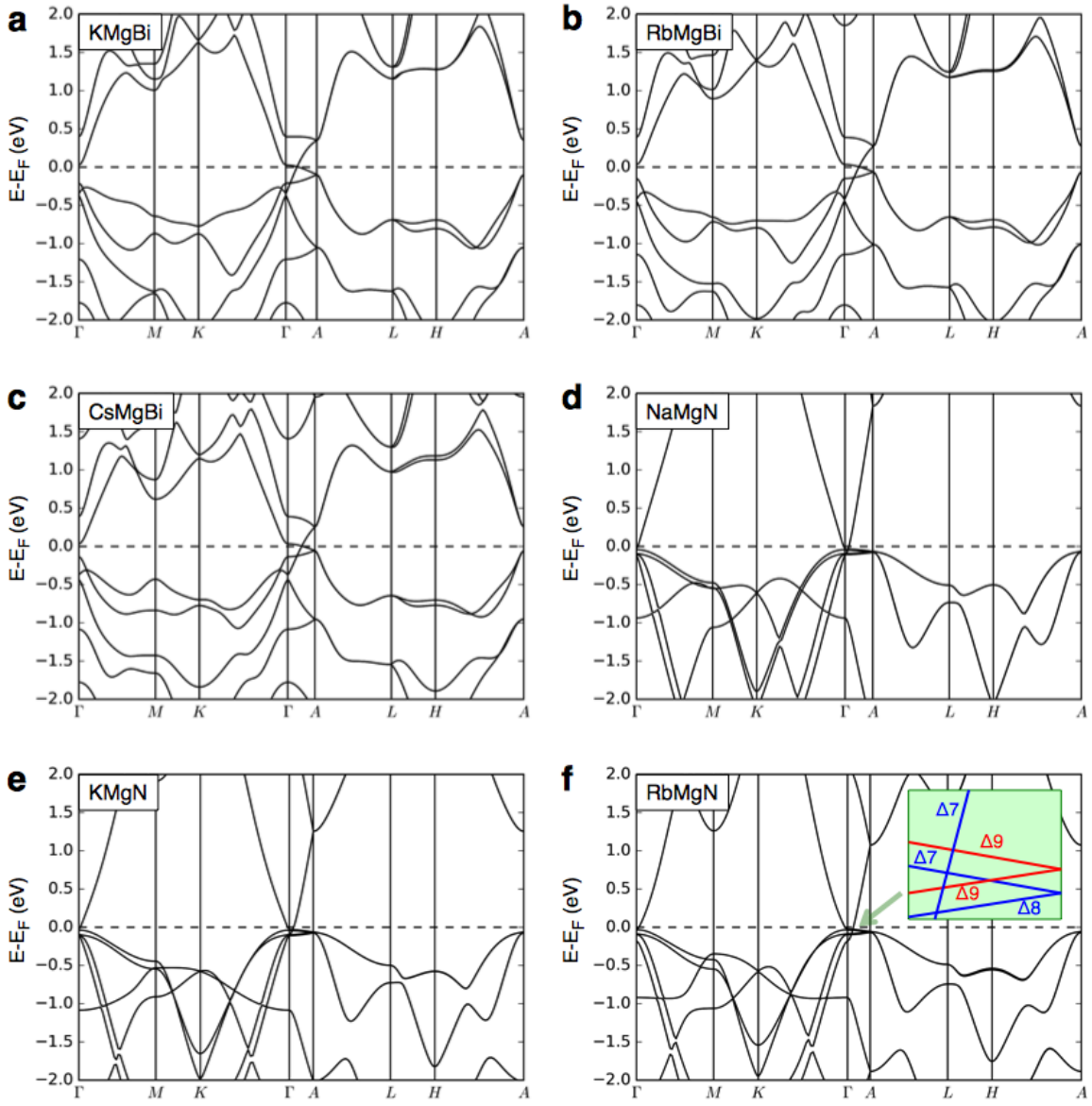

Figure S4. Electronic structures from DFT-GGA with SOC of the honeycomb structures that are the TDSM's with B = Mg. (a) Energy bands of KMgBi; (b) RbMgBi; (c) CsMgBi; (d) NaMgN; (e) KMgN; (f) RbMgN. Inset of (f) illustrates the irreducible representations of the dense states near E_f for RbMgN (common for NaMgN and KMgN).

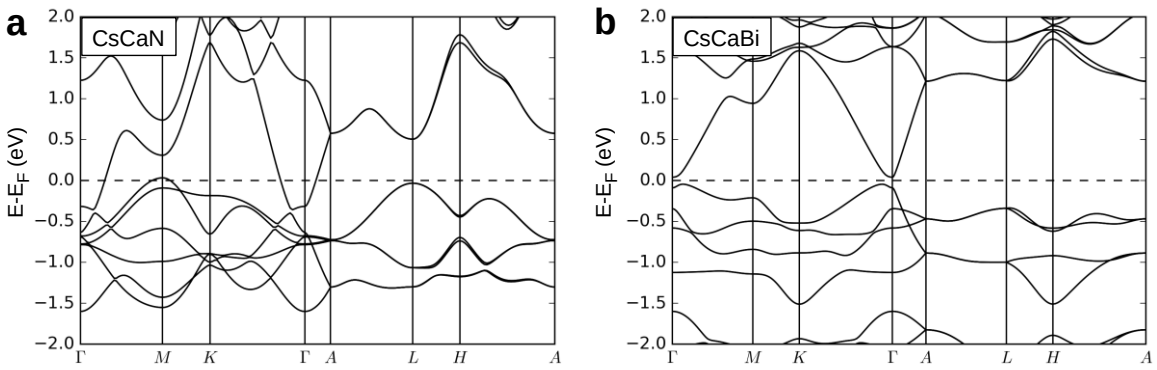

Figure S5. Electronic structures from DFT-GGA with SOC of the honeycomb structures that are the TI's with long *c* lattice constant. (a) Energy bands of CsCaN; (b) CsCaBi.

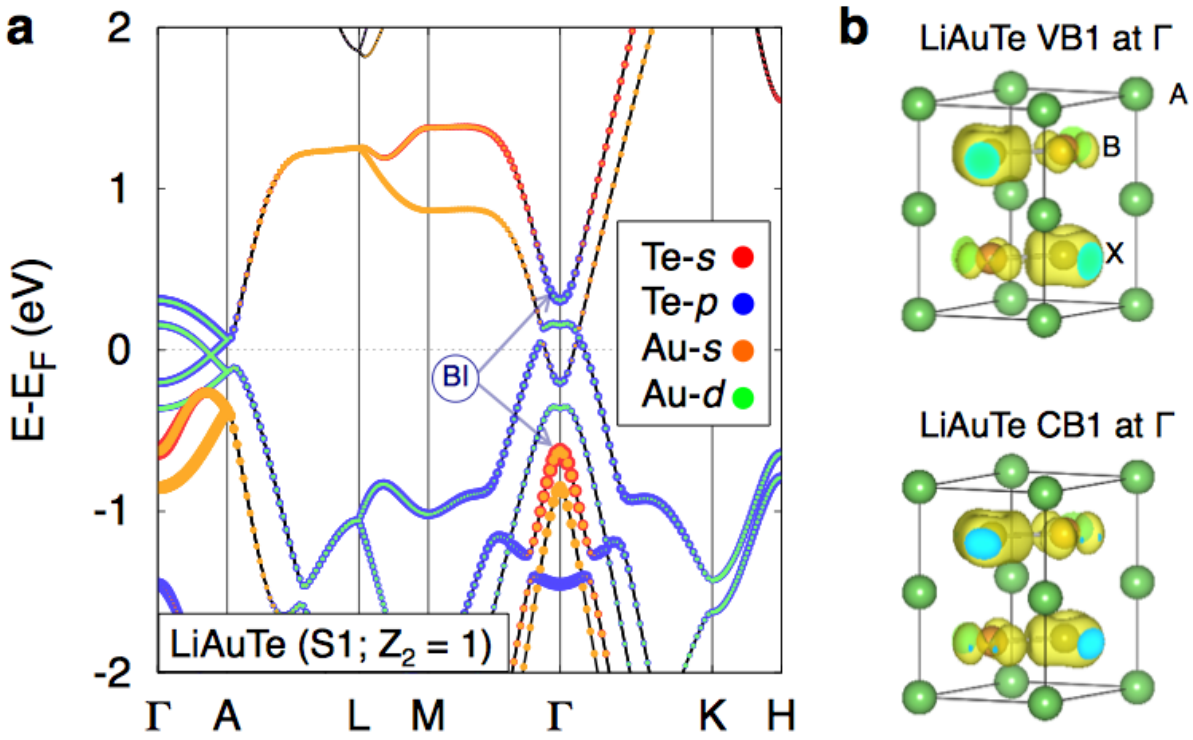

Figure S6. Electronic structures of LiAuTe in the honeycomb structure. (a) Band structure of LiAuTe from DFT-GGA with SOC. The dotted lines with different colors denote the band projection onto different atomic orbitals. The band inversion is denoted in the figure by BI, with arrows pointing to the inverted states. (b) Wave function squares of the first occupied (VB1) and first unoccupied (CB1) states in LiAuTe showing iso-surfaces at 0.15 electron/cell. The positions of the A, B, X atoms in the unit cell are denoted in (b).

B. Thermodynamic stability analysis of honeycomb TI NaCaBi

Figure S7 demonstrates the thermodynamic stability analysis of a representative stable honeycomb TI NaCaBi in the space of elemental chemical potentials ($\Delta\mu_{Na}$, $\Delta\mu_{Ca}$, and $\Delta\mu_{Bi}$). For elemental competing phases, we have $\Delta\mu_I$ (I = Na, Ca, Bi) < 0. For binary competing phases like Na_3Bi, we have $3\Delta\mu_{Na} + \Delta\mu_{Bi} < \Delta H_f$ (Na_3Bi). There is no reported ternary competing phase in this system.[3] These inequalities plus the equilibrium equation $\Delta\mu_{Na} + \Delta\mu_{Ca} + \Delta\mu_{Bi} = \Delta H_f$ (NaCaBi) define the stability region of NaCa-Bi.[4]

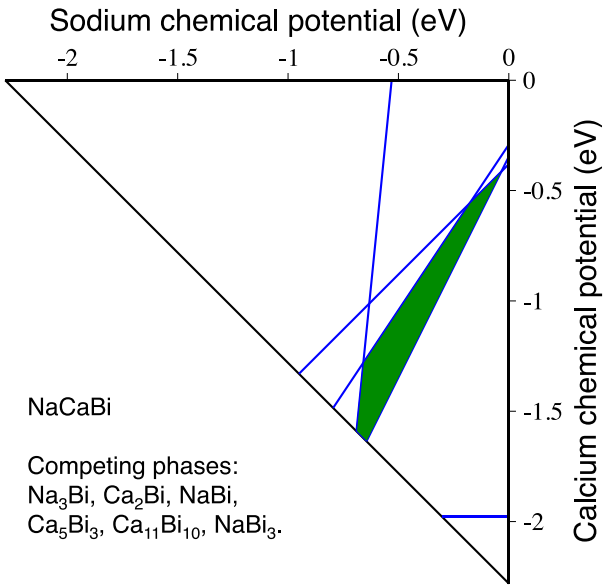

Figure S7. Stability region (in green) of NaCaBi in the space of chemical potentials. Each blue line indicates a competing phase (e.g. Na_3Bi).

C. Electronic structure of normal insulator KBaBi (S3)

Figure S8 gives the band structure of KBaBi in the S3 structure (see Figure 3b) showing a very narrow band gap of ~14 meV from DFT+SOC. The parity analysis of KBaBi (S3) gives $Z_2 = 0$. Therefore, KBaBi (S3) is a rather weak (i.e. small band gap that can be inverted by small perturbations) exception for the observed trends in Figure 3a (i.e. for the I-II-Bi compounds there, the S1, S2 and S3 structures

with a similar structure motif BiA_6B_3 are TI's, whereas the S4 and S5 structures without such motif are not TI's).

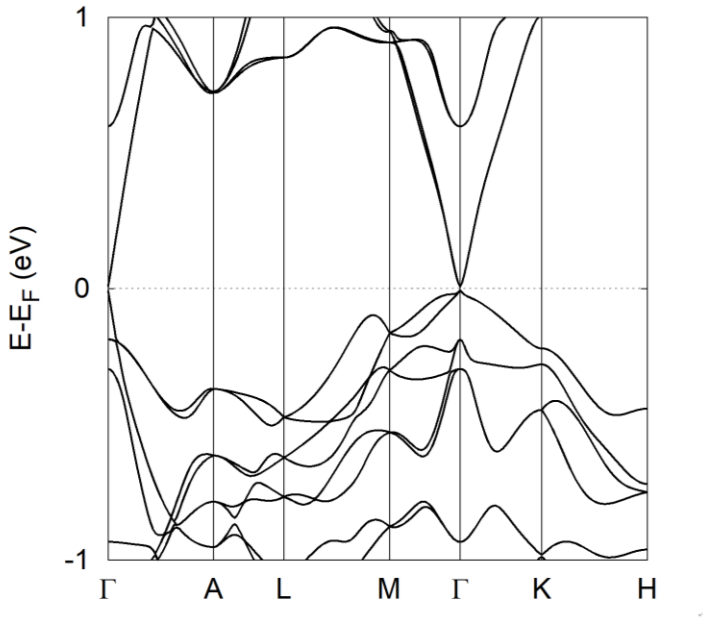

Figure S8. Electronic structure of KBaBi in the S3 structure from DFT-GGA with SOC showing a very narrow band gap (~14 meV).

IV. Double group representations of space group No. 194 ($P6_3/mmc$)

The compatibility relations between the irreducible representations of ΓA (0, 0, 0.5) and Δ (0, 0, Δ) are given in Table S2 and the character table for the double group representatives of space group $P6_3/mmc$ is given in Table S3.

Table S2. Compatibility relations between the irreducible representations of Γ, A (0, 0, 0.5) and Δ (0, 0, Δ) points for space group No. 194 ($P6_3/mmc$).

Γ/A representation	Δ representation
Γ_7^+, Γ_7^-	$\rightarrow \quad \Delta_7$
Γ_8^+, Γ_8^-	$\rightarrow \quad \Delta_8$
Γ_9^+, Γ_9^-	$\rightarrow \quad \Delta_9$
$A_4 + A_5$	$\rightarrow \quad 2\Delta_9$
A_6	$\rightarrow \quad \Delta_7 + \Delta_8$

Table S3. Character table for the double group representatives of space group $P6_3/mmc$ (D_{6h}) for the high symmetry Γpoint in the Brillouin zone.

D_{6h}	E	$\bar{E}$	C_2	$2C_3$	$2\bar{C}_3$	$2C_6$	$2\bar{C}_6$	$3C'_2$	$3C''_2$	I	$\bar{I}$	σ_h	$2S_6$	$2\bar{S}_6$	$2S_3$	$2\bar{S}_3$	$3\sigma_d$	$3\sigma_v$
Γ_7^+	2	-2	0	1	-1	$\sqrt{3}$	$-\sqrt{3}$	0	0	2	-2	0	1	-1	$\sqrt{3}$	$-\sqrt{3}$	0	0
Γ_7^-	2	-2	0	1	-1	$-\sqrt{3}$	$\sqrt{3}$	0	0	2	-2	0	1	-1	$-\sqrt{3}$	$\sqrt{3}$	0	0
Γ_8^+	2	-2	0	-2	2	0	0	0	0	2	-2	0	-2	2	0	0	0	0
Γ_8^-	2	-2	0	1	-1	$\sqrt{3}$	$-\sqrt{3}$	0	0	-2	2	0	-1	1	$-\sqrt{3}$	$\sqrt{3}$	0	0
Γ_9^+	2	-2	0	1	-1	$-\sqrt{3}$	$\sqrt{3}$	0	0	-2	2	0	-1	1	$\sqrt{3}$	$-\sqrt{3}$	0	0
Γ_9^-	2	-2	0	-2	2	0	0	0	0	-2	2	0	2	-2	0	0	0	0

References

(1) Heyd, J.; Scuseria, G. E.; Ernzerhof, M. *J. Chem. Phys.* **2003**, *118*, 8207.
(2) Heyd, J.; Scuseria, G. E.; Ernzerhof, M. *J. Chem. Phys.* **2006**, *124*, 219906.
(3) McCalla, E.; Abakumov, A. M.; Saubanère, M.; Foix, D.; Berg, E. J.; Rousse, G.; Doublet, M.-L.; Gonbeau, D.; Novák, P.; Van Tendeloo, G.; Dominko, R.; Tarascon, J.-M. *Science* **2015**, *350*, 1516.
(4) Zhang, X.; Yu, L.; Zakutayev, A.; Zunger, A. *Adv. Funct. Mater.* **2012**, *22*, 1425.
(5) Fu, L.; Kane, C. L.; Mele, E. J. *Phys. Rev. Lett.* **2007**, *98*, 106803.
(6) Yang, B.-J.; Nagaosa, N. *Nature Communications* **2014**, *5*, 4898.
(7) Fu, L.; Kane, C. L. *Phys. Rev. B* **2006**, *74*, 195312.
(8) Yu, R.; Qi, X. L.; Bernevig, A.; Fang, Z.; Dai, X. *Phys. Rev. B* **2011**, *84*, 075119.
(9) Zhang, H. J.; Chadov, S.; Müchler, L.; Yan, B.; Qi, X. L.; Kübler, J.; Zhang, S. C.; Felser, C. *Phys. Rev. Lett.* **2011**, *106*, 156402.